Received March 10, 2021, accepted March 25, 2021, date of publication March 31, 2021, date of current version April 9, 2021.

Digital Object Identifier 10.1109/ACCESS.2021.3070047

Balancing Method Based on Flyback Converter for Series-Connected Cells

YILIN CAO, KAI LI, AND MIN LU
School of Mechanical and Electrical Engineering, Shihezi University, Xinjiang 832007, China

Corresponding author: Min Lu (lm_mac@shzu.edu.cn)

This work was supported in part by the High-Level Talents Program of Shihezi University under Grant RCZK202005, and in part by the International Cooperation Project of Shihezi University under Grant GJHZ202003.

ABSTRACT For the various imbalances of series-connected cells, the existing balancing methods has the disadvantages of limited energy flow direction and unnecessary charge transfer. Based on flyback converter, this paper proposes a multi-winding input and multi-winding output bi-directional equalization topology. It can realize any cell (s) to any cell (s) balancing, which has the advantage of flexible balancing energy flow path. This paper adopts the control strategy of time-sharing participation in equalization according to the order of the initial state of charge (SOC) of cells, it can solve the problem of unnecessary energy transfer and simplify the control logic. In addition, it gets rid of the influence of energy loss of the circuit components on the setting of the fixed equalization end judgment value, whether equalization ends or not depends on the difference between the discharge cells and the charge cells in this paper, which has the advantage of random adaptive adjustment. In this paper, the operational principle of the proposed circuit are analyzed and the equalization strategy is described in detail. A comparison in balancing performance between the conventional equalization topology based on flyback converter and proposed topology is shown in static state. To verify the validity of the proposed method, the simulation experiment of four cells series-connected is carried out, and the simulation results show that the balancing method proposed in this paper has faster equalization speed and higher equalization energy transfer efficiency.

INDEX TERMS Any cell(s) to any cell(s), balancing method, flyback converter, series-connected cells, time-sharing.

I. INTRODUCTION

Lithium-ion batteries have the advantages of high power and energy density, low self-discharge rate, no memory effect, long life cycle, no pollution, etc. It is widely used in various equipment [1], [2], however, the single cell voltage of lithium-ion battery is low, only 3.6V. In order to meet the demand of voltage level in practical application, it is usually necessary to use multiple single cells in series. Due to the limitation of cells manufacturing process and the influence of cells operating environment, there are inconsistencies of internal resistance, self-discharge rate, capacity and other parameters between cells [3]. After multiple cycles of charge and discharge, the inconsistencies are gradually amplified. It can lead to overcharge and discharge of individual cells, which decreases usable capacity, shortens lifetime and even worse causes safety problems, such as explosion and spontaneous combustion [4]. Therefore, it is of great significance to study the balancing method of series-connected cells, which can reduce the inconsistencies, improve the batteries capacity utilization, extend the batteries life cycle and ensure the safe and efficient operation of the batteries [5].

Currently, balancing methods are mainly divided into two categories: dissipative balancing and non-dissipative balancing [6], [7]. The essence of dissipative balancing is to convert electric energy into heat energy through a bypass resistor, and dissipate the deviation energy between cells [8], which has the problems of a lot of energy loss and thermal management. Non-dissipative balancing uses energy storage elements, such as capacitors, inductors, and transformers to transfer energy from the strongest cells to the weakest cells, which has the advantages of low energy loss and high equalization efficiency [9]. With the development of power electronics technology and the improvement of energy conservation requirements, non-dissipative balancing method has become a hot research topic at home and abroad [10].

The associate editor coordinating the review of this manuscript and approving it for publication was Zheng Chen.

The following is a classification of non-dissipative balancing method according to different energy transfer paths.

Cell to pack [11]–[13], the energy of the high-energy cells is released to the batteries. It can effectively prevent the overcharge of the high- energy cells. Pack to cell [14], [15] is to transfer the energy of the batteries to the low-energy cells, which can avoid the over-discharge of the low-energy cells. Cell to pack to cell [16]–[19] combines the advantages of cell to pack and pack to cell, and realizes the bidirectional balancing between batteries and cell. Although the above balancing methods can solve the problem of overcharge and over-discharge of some cells, there is unnecessary charge transfer, which affects the life of batteries.

Cell to part of the pack [20], part of the pack to cell [21], Cell to part of the pack to cell [22], compared with the balancing between cell and batteries, although they solve the problem of coexistence of charge and discharge of some cells in equalization, the direction of energy flow is limited. Energy flows either upstream or downstream of a certain cell. The equalization speed is directly related to the number of cells upstream and downstream.

Adjacent cell to cell [23]–[27], when the unbalanced cells are adjacent to each other, the transfer efficiency is high and the equalization speed is fast. However, when the unbalanced cells are far away from each other, the equalization transfer path is long, the equalization speed is slow and the energy loss is high. Direct cell-to-cell [28]–[30], which is usually realized by a common energy storage element, such as capacitor, inductor and transformer. It can realize the direct balancing between the highest energy cell and the lowest energy cell, and obtain higher equalization efficiency. However, this method can only achieve the balancing between two cells at the same time, and has complex control logic.

To sum up, the existing equalization methods have certain limitations in energy transfer between cells. Based on flyback converter, this paper proposes a bidirectional balancing topology with multi-winding input and multi-winding output. Compared with adjacent cell to cell balancing topology, the energy transfer path is no longer affected by the location of cells, it can achieve direct balancing between any cells and solve the problem of long-distance turnover energy between cells that are far away each other. Compared with direct cell to cell balancing topology, it can achieve the balancing between multiple pairs of cells at the same time. Compared with cell to part of the pack to cell balancing topology, balancing energy flow direction is more flexible and rich. Compared with cell to pack to cell balancing topology, it solves the problem that charge and discharge of the same cells coexist during the equalization process, and improves the life cycle of the batteries. In this paper, the operational principles of balancing topology are explained and the equalization strategy is demonstrated. A comparison in balancing performance between the conventional equalization topology based on flyback converter and proposed topology is shown in static state. The simulation experiment of four cells series-connected is implemented and the simulation experimental results demonstrate the effectiveness of the balancing method proposed in this paper.

II. STRUCTURE OF BALANCING SYSTEM

According to the difference of SOCs among cells, the inconsistencies of series-connected cells can be generally divided into four types: one highest cell in the string (referred to as: one highest) as shown in Figure 1(a); one highest and one lowest cell (referred to as: one highest and one lowest) as shown in Figure 1(b); some high cells and some low cells(referred to as: some high and some low) as shown in Figure 1(c); one lowest cell in the string(referred to as: one lowest) as shown in Figure 1(d). In this paper, a novel balancing method with three equalization modes is proposed, which can solve different imbalances and improve the accuracy of balancing.

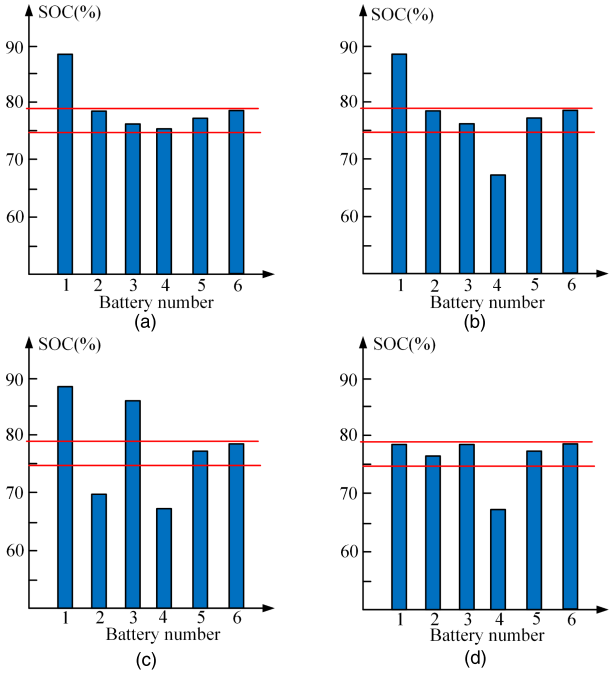

FIGURE 1. Series-connected cells imbalanced types. (a) One highest. (b) One highest and one lowest. (c) Some high and some low. (d) One lowest.

The structure diagram of the balancing system proposed in this paper is shown in Figure 2. The three balancing modes: one highest balancing mode, some high and some low balancing mode, and one lowest balancing mode. The some high and some low balancing mode aims to solve the inconsistencies of one highest and one lowest, and some high and some low. During the work process, multiple balancing modes can be switched automatically. The balancing system is composed of batteries, balancing circuit, SOC estimation module and microcontroller. The balancing circuit consists of a multi-input, multi-output bidirectional flyback converter. The SOC of single cell is estimated by ampere-hour integration method in real time. Compared and calculated the collected

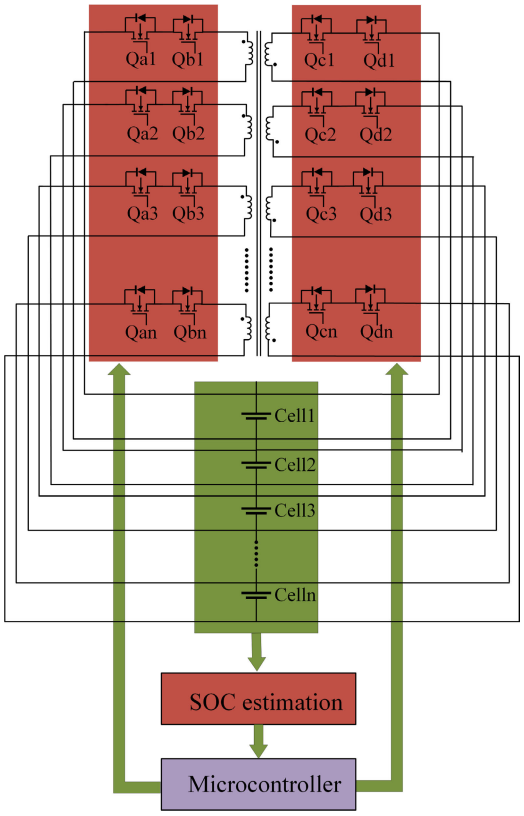

FIGURE 2. Structure diagram of equalization control system.

SOC values of each cell, then the microcontroller controls the MOSFETs on and off.

Each cell has two optional transformer windings, each winding is connected in series with two MOSFETs. By controlling the on-off combination of the two MOSFETs, the energy can flow in or out, realizing the bidirectional flow of energy. For the convenience of control, it is stipulated that the left side of the transformer is used as the discharge of high-energy cells, and the right side of the transformer is used as the charge of low-energy cells. When the energy on the left side of the transformer transfers to the right side, MOSFETs Q_{ai}, Q_{ci} turn on, Q_{bi}, Q_{di} turn off. The switches of Q_{ai} and Q_{ci} and the diodes of Q_{bi} and Q_{di} work together to achieve unidirectional current flow and prevent current from flowing back to the high SOC cell side; when high-energy cell needs discharge, the two MOSFETs in the winding circuit on the right side of the transformer are turned off; otherwise, the two MOSFETs in the winding circuit on the left side of the transformer are turned off. All MOSFETs are controlled by a pair of complementary PWM signals, which greatly reduces the number of control signals and complexity of the MOSFETs drive circuit. The equalization circuit has high flexibility, which can realize the equalization of any cell(s) to any cell(s).

III. OPERATING PRINCIPLE OF EQUALIZATION CIRCUIT

Since this paper uses a multi-input and multi-output bidirectional flyback DC converter, the magnetic flux of magnetic core needs to be restored to the original size, reducing electromagnetic interference during each switching cycle. In the discontinuous current mode (DCM), all the energy stored in the transformer inductor is released in each switching cycle, which can reset the magnetic flux, effectively avoid electromagnetic saturation and improve the energy utilization rate. Therefore, the flyback converter designed in this paper works in the discontinuous current mode.

Taking $Cell_1$ and $Cell_2$ as an example, as shown in Figure 3, assuming that $SOC_1 > SOC_2$, the equalization circuit transfers the energy from $Cell_1$ to $Cell_2$, and its working principle is analyzed below. In order to simplify the analysis, the following assumptions are made: the parasitic parameters of components and circuits are ignored; the cell terminal voltage is constant in a switching cycle.

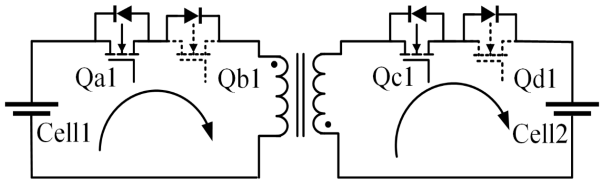

FIGURE 3. Energy transfer from $Cell_1$ to $Cell_2$.

The transformer is used as an energy storage element to transfer energy. During an equalization period, the primary loop and the secondary loop of the transformer are turned on alternately. The working process can be divided into two modes. Where D is the PWM duty cycle, and T is the switching period. The key waveform of energy transfer from $Cell_1$ to $Cell_2$ is shown in Figure 4.

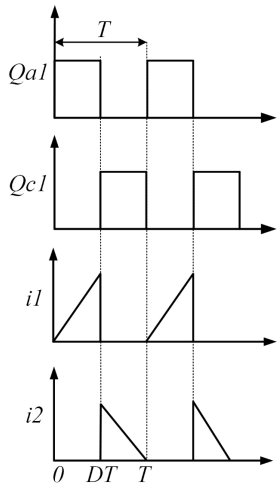

FIGURE 4. Key waveform of energy transfer from $Cell_1$ to $Cell_2$.

Mode 1$[0 - DT]$, Q_{a1} is on, Q_{c1}, Q_{b1}, Q_{d1} are off, $Cell_1$ discharges, the primary inductor of the transformer stores energy, and the upper side of primary winding is positive and the lower side is negative. The equivalent circuit model of $Cell_1$ discharging loop is shown in Figure 5.

In the model shown in Figure 5, U_1 is the voltage of $Cell_1$; L_{m1}, R_{m1} and L_1 are the magnetization inductance, magnetization resistance and leakage inductance of the primary winding; R_1 is the equivalent resistance of the primary loop; U_s is the on voltage drop of MOSFET. Taking the current direction in the Figure 5 as positive, it can be obtained from Kirchhoff's voltage law and current law:

$$\begin{cases} i_1 R_1 + U_s + L_1 \dfrac{di_1}{dt} + i_{Rm} R_{m1} = U_1 \\ L_{m1} \dfrac{di_{Lm}}{dt} = i_{Rm} R_{m1} \\ i_1 = i_{Rm} + i_{Lm} \end{cases} \tag{1}$$

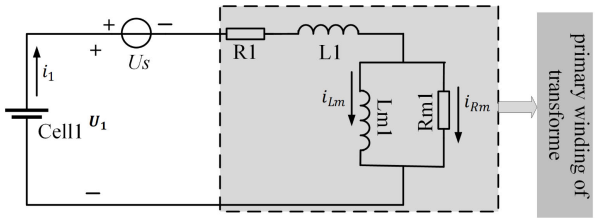

FIGURE 5. Equivalent circuit of $Cell_1$ discharging loop.

E_{U_1} is the energy released by $Cell_1$, $E_{L_{m1}}$ is the energy absorbed by the primary winding of the transformer, E_{U_s}, E_{R_1}, E_{L_1}, $E_{R_{m1}}$ are the losses of MOSFET, the equivalent resistance of primary loop, leakage inductance of the primary winding and magnetization resistance of the primary winding. According to the law of conservation of energy:

$$\begin{cases} E_{U_s} = \int i_1 U_s dt \\ E_{R_1} = \int {i_1}^2 R_1 dt \\ E_{R_{m1}} = \int {i_{Rm}}^2 R_{m1} dt \\ E_{L_1} = \dfrac{1}{2} L_1 {i_1}^2 \\ E_{L_{m1}} = \dfrac{1}{2} L_{m1} {i_{Lm}}^2 \\ E_{U_1} = \int i_1 U_1 dt \\ E_{U_1} = E_{U_s} + E_{R_1} + E_{L_1} + E_{L_{m1}} + E_{R_{m1}} \end{cases} \tag{2}$$

Under ideal conditions, iron loss and copper loss are ignored. At this time, the primary current i_1 is:

$$i_1 = i_{Lm} = \frac{U_1 - U_s}{L_1 + L_{m1}} t \quad (0 < t \le DT) \tag{3}$$

When $t = DT$, i_1 reaches its maximum value, and its value i_{1max} is:

$$i_{1max} = i_{Lm} = \frac{U_1 - U_s}{L_1 + L_{m1}} DT \tag{4}$$

In this process, the primary current causes the transformer core to be magnetized, and the magnetic flux increases linearly. The increase $\Delta\Phi_+$ is:

$$\Delta\Phi_+ = \frac{U_1}{N_1} DT \tag{5}$$

N_1 is the number of turns of primary winding of transformer.

The energy stored in the transformer is:

$$E_{L_{m1}} = \frac{(U_1 - U_s)^2 D^2 T^2}{2L_{m1}(L_1 + L_{m1})^2} \tag{6}$$

Mode 2[$DT \sim T$], Q_{c1} is on, Q_{a1}, Q_{b1}, Q_{d1} are off, $Cell_2$ charges. In order to prevent the current from falling, the primary winding inductance generates the induced electromotive force with negative polarity up and positive polarity down. By magnetic coupling, the secondary winding generates the electromotive force with positive polarity up and negative polarity down. At this time, the secondary winding inductance of the transformer charges the $Cell_2$. The equivalent circuit model of $Cell_2$ charging loop is shown in Figure 6.

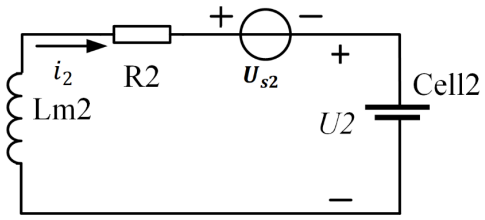

FIGURE 6. Equivalent circuit of $Cell_2$ charging loop.

In the model shown in Figure 6, U_2 is the voltage of $Cell_2$; L_{m2} and R_2 are the equivalent inductance and resistance of the secondary loop; U_{s2} is the on voltage drop of MOSFET. Taking the current direction in the Figure 6 as positive, it can be obtained from Kirchhoff's voltage law:

$$i_2 R_2 + U_2 + U_{s2} = L_{m2} \frac{di_2}{dt} \tag{7}$$

E_{U_2} is the energy absorbed by $Cell_2$, $E_{L_{m2}}$ is the energy released by the secondary winding of the transformer, $E_{U_{s2}}$ and E_{R_2} are the losses of MOSFET and equivalent resistance of the secondary loop. According to the law of conservation of energy:

$$\begin{cases} E_{R_2} = \int {i_2}^2 R_2 dt \\ E_{U_{s2}} = \int i_2 U_{s2} dt \\ E_{U_2} = \int i_2 U_2 dt \\ E_{L_{m2}} = \dfrac{1}{2} L_{m2} {i_2}^2 \\ E_{L_{m2}} = E_{U_{s2}} + E_{R_2} + E_{U_2} \end{cases} \tag{8}$$

Under ideal conditions, the decreasing slope of the secondary inductor current is:

$$\frac{di_2}{dt} = \frac{U_2 + U_{s2}}{L_{m2}} \tag{9}$$

The maximum current of secondary loop is:

$$i_{2max} = \frac{N_1 (U_1 - U_s)}{N_2 (L_1 + L_{m1})} DT \tag{10}$$

N_2 is the number of turns of secondary winding of transformer.

In this process, The secondary loop current is opposite, which has a demagnetization effect on the iron core of the transformer, and the magnetic flux decreases linearly. The reduction is:

$$\Delta\Phi_- = \frac{U_2}{N_2}(1-D)T \tag{11}$$

IV. BALANCING CONTROL STRATEGY

A. SOC ESTIMATION

The conventional method is based on the battery operating voltage. Although the battery operating voltage is easy to obtain, it is susceptible to circuit current interference, and the difference between different operating periods is large. Using SOC of cell as the basis of equalization can not only calculate the amount of charge that needs to be transferred more accurately, but also eliminate the problem of repeated charging and discharging [31]. Ampere hour integration method is a relatively simple SOC estimation method, which ignores the structure and electrical characteristics of the battery, and estimates the SOC by measuring the current of the battery during charging and discharging [32]. In the ideal case, the estimation method of ampere hour integration method is as follows:

$$SOC_{(t)} = SOC_{(t_0)} - \frac{1}{Q}\int_0^t idt \tag{12}$$

Q is the rated capacity of the battery, i is the instantaneous current of battery charging and discharging, which is positive value when discharging and negative value when charging.

B. BALANCING CONTROL STRATEGY

In the ideal situation, without considering the energy loss of circuit components, the SOC of each cell is equal to the average SOC of the batteries (SOC_d) when equalization is completed. In this paper, the SOC_d is used as the reference value to divide the unbalanced states of the batteries, and the corresponding equalization schemes are formulated according to different unbalanced states. In practical application, a certain margin can be set up above and below the SOC_d according to the circuit component parameters and electrical parameters.

$$SOC_d = \frac{1}{n}\sum_{i=1}^{n} SOC_i \tag{13}$$

n is the number of cells in the batteries.

Take four cells connected in series as an example and define $SOC_{max1} > SOC_{max2} > SOC_{min2} > SOC_{min1}$.

$$W = \begin{cases} 0, & SOC_{max1} > SOC_d > SOC_{max2} \\ & > SOC_{min2} > SOC_{min1} \\ 1, & SOC_{max1} > SOC_{max2} > SOC_d \\ & > SOC_{min2} > SOC_{min1} \\ 2, & SOC_{max1} > SOC_{max2} > SOC_{min2} \\ & > SOC_d > SOC_{min1} \end{cases} \tag{14}$$

0, *1*, and *2* represent one highest balancing mode, some high and some low balancing mode, and one lowest balancing mode, respectively. The overall flow chart of the proposed balancing method is shown in Figure 7.

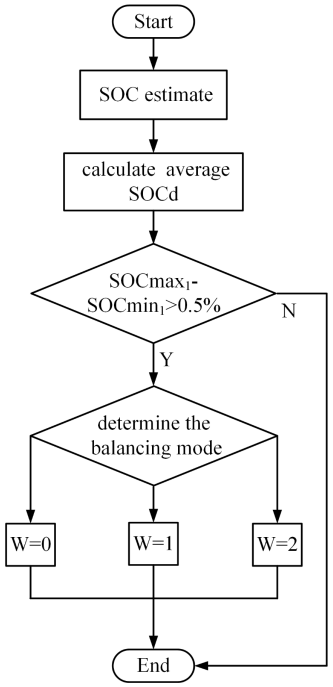

FIGURE 7. Overall flow chart of the proposed balancing method.

1) ONE HIGHEST BALANCING MODE

When $SOC_{max1} > SOC_d > SOC_{max2} > SOC_{min2} > SOC_{min1}$, the $W = 0$ balancing mode is executed. In this balancing mode, the $Cell_{max1}$ is connected to the primary side of the transformer, the $Cell_{max2}$, $Cell_{min2}$, and $Cell_{min1}$ are connected to the secondary side of the transformer. In order to avoid the coexistence of charging and discharging of the same cells during the equalization process, shortening the life of batteries, this paper strictly controls the charging and discharging actions of cells. In the $W = 0$ balancing mode, $Cell_{max1}$ only releases energy, $Cell_{max2}$, $Cell_{min2}$, and $Cell_{min1}$ only absorb energy. For the energy-absorbing cells, the corresponding MOSFETs are gradually turned on. In the process of equalization, at first, $Cell_{max1}$ transfers energy to $Cell_{min1}$, and $Cell_{max2}$ and $Cell_{min2}$ are in a waiting state. As the SOC of $Cell_{min1}$ continues to increase, the corresponding MOSFET of $Cell_{min2}$ is on when $SOC_{min1} = SOC_{min2}$, $Cell_{min2}$ starts charging at the same rate as $Cell_{min1}$. When $SOC_{min1} = SOC_{min2} = SOC_{max2}$, the corresponding MOSFET of $Cell_{max2}$ is on, $Cell_{max2}$ starts absorbing the energy released by $Cell_{max1}$ at the same rate as $Cell_{min2}$ and $Cell_{min1}$. when $SOC_{min1} = SOC_{min2} = SOC_{max2} = SOC_{max1}$, the equalization ends. Its control flow chart is shown in Figure 8.The key waveforms of $W = 0$ equalization mode depicted in Figure 9. i_{max1}, i_{max2}, i_{min2}, and i_{min1}

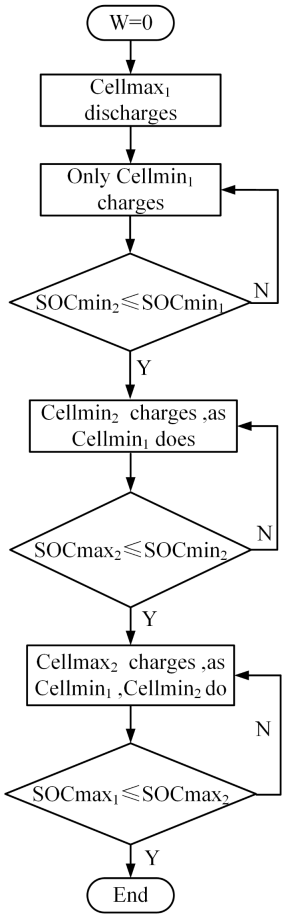

FIGURE 8. Flow chart of $W = 0$ equalization mode.

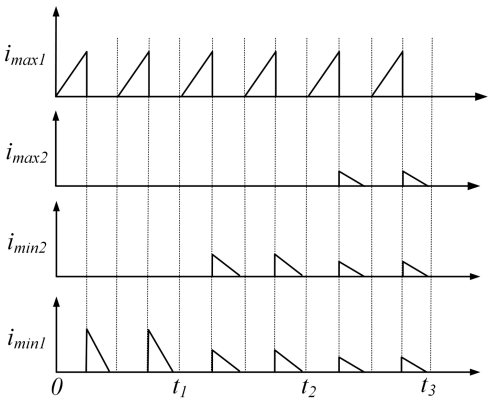

FIGURE 9. The key waveforms of $W = 0$ equalization mode.

are the equalization current of $Cell_{max}1$, $Cell_{max}2$, $Cell_{min}2$, *and* $Cell_{min}1$.

2) SOME HIGH AND SOME LOW BALANCING MODE

When $SOC_{max}1 > SOC_{max}2 > SOC_d > SOC_{min}2 > SOC_{min}1$, the $W = 1$ balancing mode is executed. In this balancing mode, the $Cell_{max}1$ and $Cell_{max}2$ are connected to the primary side of the transformer, the $Cell_{min}2$ and $Cell_{min}1$ are connected to the secondary side of the transformer. In the $W = 1$ balancing mode, $Cell_{max}1$ and $Cell_{max}2$ only releases energy, $Cell_{min}2$ and $Cell_{min}1$ only absorb energy. In the process of equalization, at first, $Cell_{max}1$ transfers energy to $Cell_{min}1$, and $Cell_{max}2$ and $Cell_{min}2$ are in a waiting state. As the energy of $Cell_{max}1$ continues to transfer, the SOC of $Cell_{max}1$ is continuously reduced. When $SOC_{max}2 = SOC_{max}1$, the corresponding MOSFET of $Cell_{max}2$ is on, $Cell_{max}2$ starts releasing energy at the same rate as $Cell_{max}1$. At the same time, the SOC of $Cell_{min}1$ continues to increase. When $SOC_{min}1 = SOC_{min}2$, the corresponding MOSFET of $Cell_{min}2$ is on, $Cell_{min}2$ starts charging at the same rate as $Cell_{min}1$. When $SOC_{min}1 = SOC_{min}2 < SOC_{max}2 = SOC_{max}1$, $Cell_{max}2$ and $Cell_{max}1$ transfer energy to $Cell_{min}2$ and $Cell_{min}1$. When $SOC_{min}1 = SOC_{min}2 = SOC_{max}2 = SOC_{max}1$, the balancing ends. Its control flow chart is shown in Figure 10. The key waveforms of $W = 1$ equalization mode depicted in Figure 11.

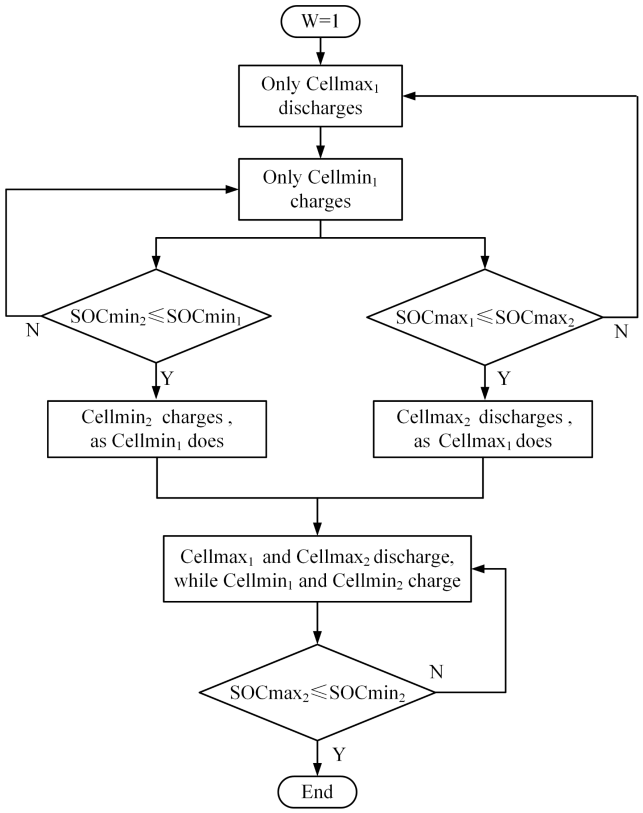

FIGURE 10. Flow chart of $W = 1$ equalization mode.

3) ONE LOWEST BALANCING MODE

When $SOC_{max}1 > SOC_{max}2 > SOC_{min}2 > SOC_d > SOC_{min}1$, the $W = 2$ balancing mode is executed. In this balancing mode, the $Cell_{max}1$, $Cell_{max}2$ and $Cell_{min}2$ are connected to the primary side of the transformer, and the $Cell_{min}1$ is connected to the secondary side of the transformer. In the $W = 2$ balancing mode, $Cell_{max}1$, $Cell_{max}2$, and $Cell_{min}2$ only release energy, $Cell_{min}1$ only absorb energy. For the energy- releasing cells, the corresponding MOSFETs are gradually turned on. In the process of equalization, at first,

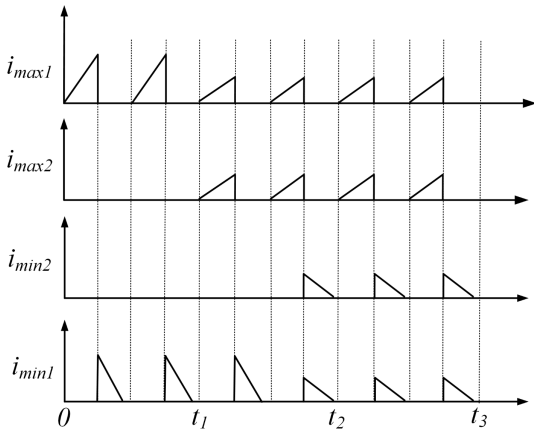

FIGURE 11. The key waveforms of $W = 1$ equalization mode.

$Cell_{max1}$ transfers energy to $Cell_{min1}$, and $Cell_{max2}$ and $Cell_{min2}$ are in a waiting state. As the SOC of $Cell_{max1}$ continues to decrease, the corresponding MOSFET of $Cell_{max2}$ is on when $SOC_{max2} = SOC_{max1}$, $Cell_{max2}$ starts discharging at the same rate as $Cell_{max1}$. When $SOC_{max2} = SOC_{max1} = SOC_{min2}$, the corresponding MOSFET of $Cell_{min2}$ is on, $Cell_{min2}$ starts releasing the energy at the same rate as $Cell_{max2}$ and $Cell_{max1}$. When $SOC_{min1} = SOC_{min2} = SOC_{max2} = SOC_{max1}$, the equalization ends. Its control flow chart is shown in Figure12. The key waveforms of $W = 2$ equalization mode depicted in Figure 13.

By increasing the number of charging and discharging cells in time-sharing manner, the cells with high SOC are always in a discharging state, and the cells with low SOC are always in the charging state. In this way, the coexistence of charge and discharge of the same cells in a balancing process is effectively avoided. The initial balancing time sequence is determined by the order of the initial SOC of cells, and the control logic is simple and rigorous. Whether equalization ends or not depends on the difference between the discharged cells and the charged cells in this paper, which has the advantage of random adaptive adjustment. In addition, it gets rid of the influence of energy loss of the circuit components on the setting of the fixed equalization end judgment value. The balancing current is adjusted by controlling the duty cycle of the MOSFET. In this paper, a constant duty cycle is adopted and the maximum discharge current is 0.5C. In the balancing process, with the increase of cells on the side of primary and secondary windings, secondary windings, the balancing loop is shunted.

V. SIMULATION RESULTS AND ANALYSIS

In order to verify the effectiveness of the balancing method proposed in this paper, four cells series-connected equalization model is built. The model uses the Simscape battery model and MOSFETs to simulate the power circuit. The controller was implemented as an embedded MATLAB function. The static equalization, charge equalization, and discharge equalization simulation experiments are

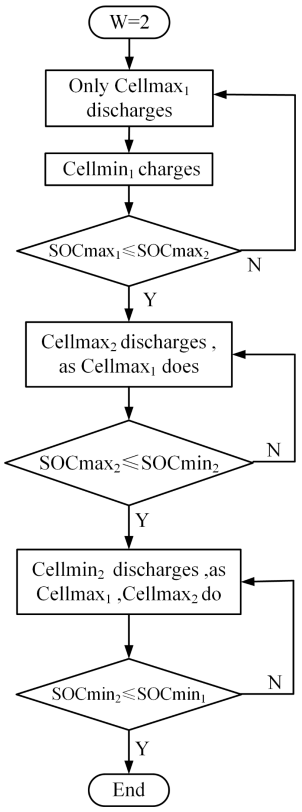

FIGURE 12. Flow chart of $W = 2$ equalization mode.

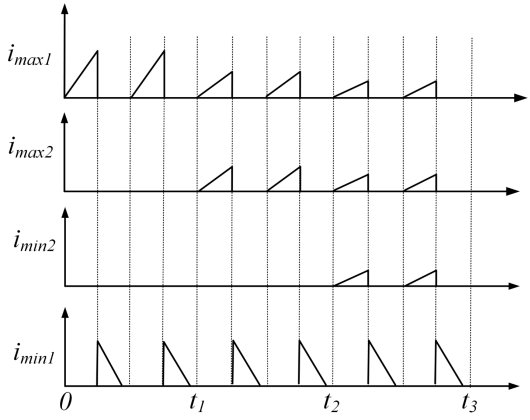

FIGURE 13. The key waveforms of $W = 2$ equalization mode.

performed respectively. This paper mainly analyzes the static equalization simulation experiments in detail. The specific parameters of the simulation model are shown in Table 1.

Compared with conventional topology based on flyback converter [33], [34] in static equalization. The conventional equalization topology circuit is shown in Figure 14. The two topologies set the same initial SOCs and transformer parameters. The initial SOCs set in static equalization are shown in Table 2. The change of SOCs of cells in the simulation are shown in Figures 15, 16, and 17.

According to the SOC at the beginning and the end of equalization to do a comparative analysis of energy

TABLE 1. Simulation parameters.

Parameter name	Value
rated voltage of single cell	3.6 V
rated capacity of single cell	6.5A.h
switch frequency	10 kHz
inductance of primary winding	48 uH
inductance of secondary winding	48 uH
MOS voltage drop	0.6 V
PWM duty cycle	50%
transformer turn ratio	1 :1

TABLE 2. The initial SOC of cells in the static state.

	$Cell_1$	$Cell_2$	$Cell_3$	$Cell_4$
one highest	92.76%	84.49%	83.46%	85.52%
some high and some low	92.76%	83.46%	89.66%	85.52%
one lowest	92.76%	91.73%	90.69%	86.56%

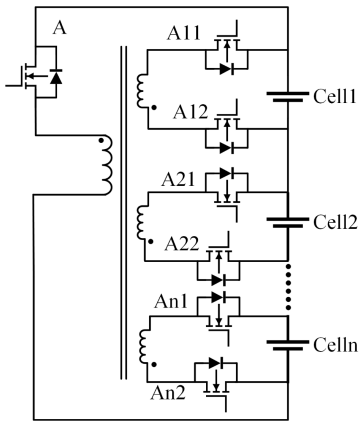

FIGURE 14. The conventional equalization topology circuit.

efficiency, η is the equalization efficiency, n is the number of cells, SOC_i is the initial state of charge, SOC_e is the state of charge after equalization, then

$$\eta = \frac{nSOC_e}{\sum_{i=1}^{n} SOC_i} \tag{15}$$

The comparison of equalization time and energy efficiency of the two topologies in the static state are shown in Table 3.

Compared with the conventional equalization topology, the equalization speed in this paper is increased by 2-3 times, and the equalization efficiency is improved by more than 0.4%. The energy flow path of the balancing circuit proposed in this paper is flexible. It can realize any cell (s) to any cell (s) balancing. Under one highest imbalance, the cells with low SOC charge in time-sharing manner in this paper, while the cells with low SOC charge simultaneously in conventional topology, which leads to the phenomenon that

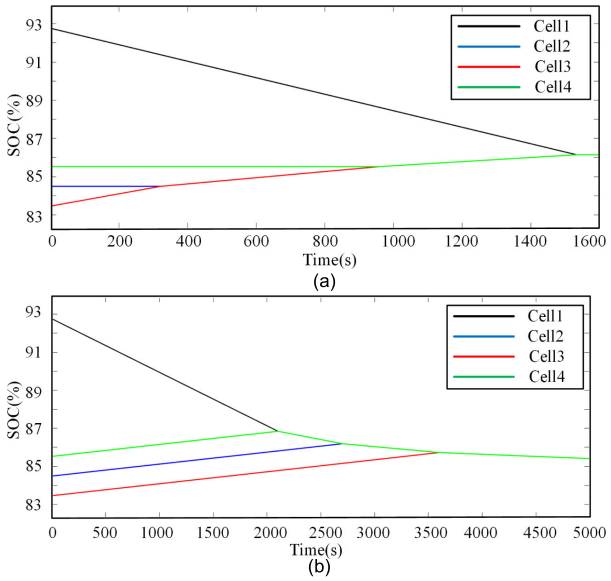

FIGURE 15. Battery SOC change process under one highest imbalance. (a) the proposed topology. (b) the conventional topology.

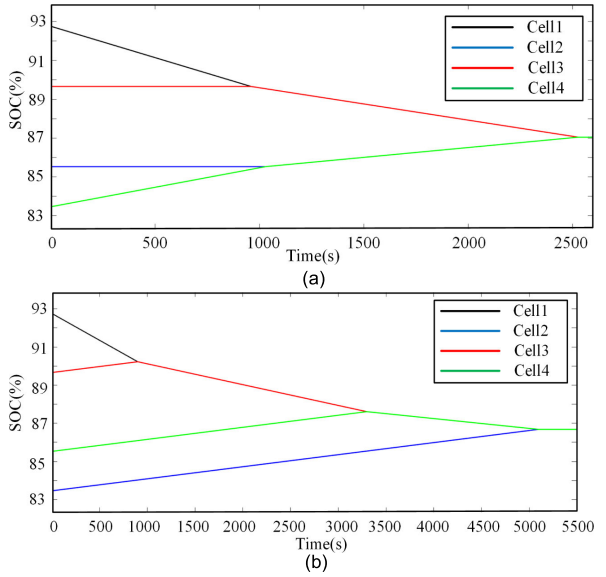

FIGURE 16. Battery SOC change process under some high and some low imbalance. (a) the proposed topology. (b) the conventional topology.

some cells charge first and then discharge. Under some high and some low imbalance, the cells with low SOC charge in time-sharing manner and the cells with high SOC discharge in time-sharing manner in this paper, while unnecessary discharge operations are performed on cells with lower SOC, and unnecessary charging operations are performed on cells with higher SOC in conventional topology. Under one lowest imbalance, the cells with high SOC discharge in time-sharing way in this paper, while the cells with high SOC discharge at the same time in conventional topology, which leads to the phenomenon that some cells discharge first and then charge. Through the above comparison, it can be found that the

TABLE 3. Comparison of two equalization topologies.

	one highest		some high and some low		one lowest	
	the proposed topology	the conventional topology	the proposed topology	the conventional topology	the proposed topology	the conventional topology
balancing time	1531s	3602s	2523s	5094s	1629s	4474s
Balancing efficiency	99.52%	99.04%	99.07%	98.67%	99.36%	98.61%

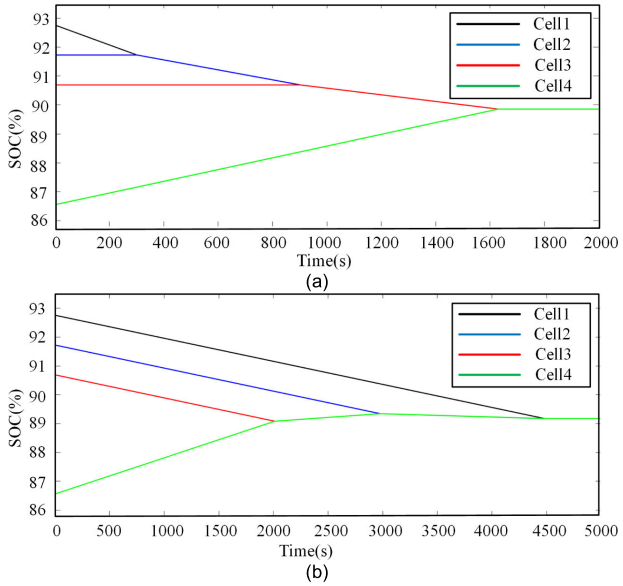

FIGURE 17. Battery SOC change process under one lowest imbalance. (a) the proposed topology. (b) the conventional topology.

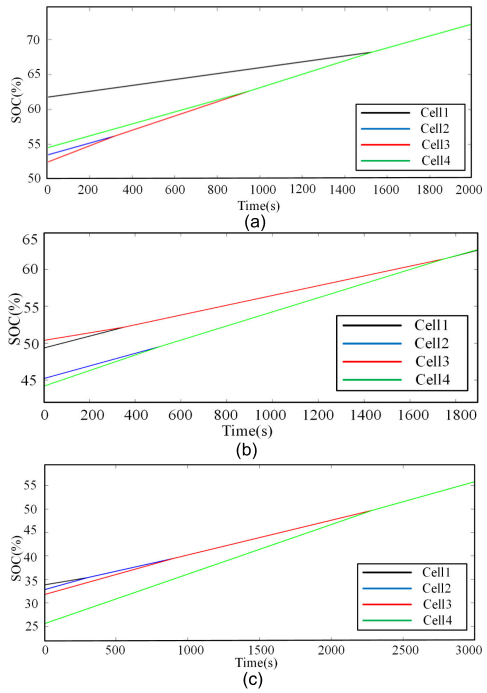

FIGURE 18. Battery SOC change process in the charging state. (a) One highest. (b) Some high and some low. (c) One lowest.

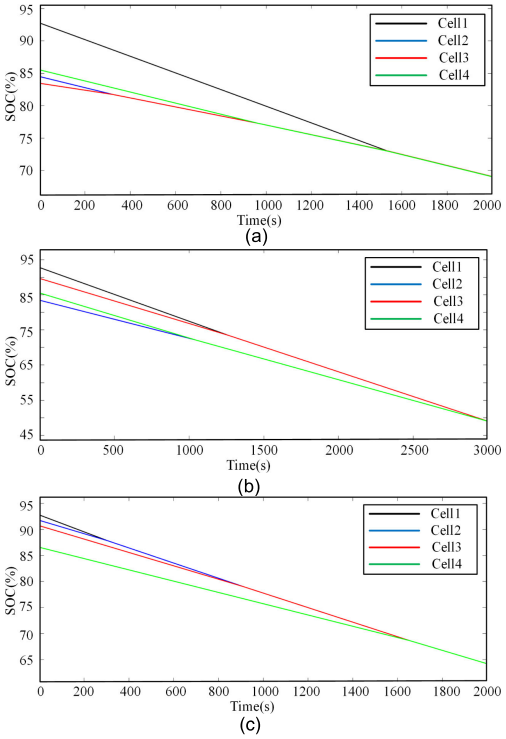

FIGURE 19. Battery SOC change process in the discharging state. (a) One highest. (b) Some high and some low. (c) One lowest.

TABLE 4. The initial SOC of cells in the charging state.

	$Cell_1$	$Cell_2$	$Cell_3$	$Cell_4$
one highest	61.75%	53.47%	52.44%	54.52%
some high and some low	49.33%	45.20%	50.37%	44.17%
one lowest	33.82%	32.79%	31.76%	25.56%

balancing method proposed in this paper significantly avoids the repeated charging and discharging of cells, reduces the loss of energy in the transfer process, improves the energy utilization rate and prolongs life cycle of batteries.

Simulation verification in the charging state, the constant current source is set to 2 A. The initial SOCs set in charging state is shown in Table 4. The change of SOCs of cells in the simulation are shown in Figures 18.

Simulation verification in the discharging state, the constant current source is set to −3 A. The initial SOCs set in charging state is shown in Table 2. The change of SOCs of cells in the simulation are shown in Figures 19.

It can be seen from Figure 18 and Figure 19 that the proposed equalization method can quickly reach SOC equalization in the charging and discharging states. In the charging state, it effectively suppresses the overcharging of cells with high SOC; in the discharging state, it effectively suppresses the over-discharge of cells with low SOC, which can improve the overall performance of the batteries.

VI. CONCLUSION AND FUTURE WORK

According to the classification of batteries imbalances, this paper proposes a novel balancing method with three equalization modes, which can solve different imbalances in a targeted manner, and improve the accuracy of balancing. The equalization method proposed in this paper is based on the flyback converter, which is a multi-winding input and multi-winding output bi-directional equalization topology, it can realize the balancing of multiple pairs of any cell to any cell at the same time, and the equalization paths are flexible. For the different imbalance states, the corresponding balancing rule is formulated. Adopting the control strategy of time-sharing participation in balancing, it solves the problem of unnecessary energy transfer. The initial balancing time sequence is determined by the order of the initial SOC of cells, and the control logic is simple and rigorous. In addition, it gets rid of the influence of energy loss of the circuit components on the setting of the fixed equalization end judgment value, whether equalization ends or not depends on the difference between the discharged cells and the charged cells in this paper, which has the advantage of random adaptive adjustment. In this paper, the operational principle of equalization circuit are analyzed and control strategy are presented in detail. Compared with conventional topology based on flyback converter, the equalization speed in this paper is increased by 2-3 times, and the equalization efficiency is improved by more than 0.4%. It can be seen that the equalization speed and efficiency of this paper have significant advantages.

At the same time, the balancing method proposed in this paper also has the following shortcomings: due to the limitation of transformer hardware structure, the number of cells that can be equalized by a single transformer is limited; In the process of equalization, there will be occasional peak current. In the future, further research on buffer circuit can be done to improve the stability of the equalization circuit.

REFERENCES

[1] N. Xue, W. Du, T. A. Greszler, W. Shyy, and J. R. R. A. Martins, "Design of a lithium-ion battery pack for PHEV using a hybrid optimization method," *Appl. Energy*, vol. 115, pp. 591–602, Feb. 2014.
[2] L. Lu, X. Han, J. Li, J. Hua, and M. Ouyang, "A review on the key issues for lithium-ion battery management in electric vehicles," *J. Power Sources*, vol. 226, pp. 272–288, Mar. 2013.
[3] Y. Chunlei and L. Zhiyuan, "Equalization control method design for power batteries in an electric vehicle," *J. Shanghai Jiaotong Univ.*, vol. 45, no. 8, p. 1186, 2011.
[4] Y. Lingyun, Z. Xing, H. Tiantian, Z. Zhijuan, and S. Kaichen, "Research on active balance technology of power battery pack based on multi-transformer method," *Chin. J. Sci. Instrum.*, vol. 39, no. 7, pp. 83–91, 2018.
[5] H. C. Lin, Y. J. He, and C. W. Liu, "Design of an efficient battery charging system based on ideal multi-state strategy," in *Proc. Int. Symp. Comput., Consum. Control (ISC)*, Jul. 2016, pp. 956–959.
[6] C. Pinto, J. V. Barreras, E. Schaltz, and R. E. Araujo, "Evaluation of advanced control for Li-ion battery balancing systems using convex optimization," *IEEE Trans. Sustain. Energy*, vol. 7, no. 4, pp. 1703–1717, Oct. 2016.
[7] M.-Y. Kim, J.-H. Kim, and G.-W. Moon, "Center-cell concentration structure of a cell-to-cell balancing circuit with a reduced number of switches," *IEEE Trans. Power Electron.*, vol. 29, no. 10, pp. 5285–5297, Oct. 2014.
[8] S. Zhang, J. Qiang, L. Yang, and X. Zhao, "Prior-knowledge-independent equalization to improve battery uniformity with energy efficiency and time efficiency for lithium-ion battery," *Energy*, vol. 94, pp. 1–12, Jan. 2016.
[9] X. Zheng, X. Liu, Y. He, and G. Zeng, "Active vehicle battery equalization scheme in the condition of constant-voltage/current charging and discharging," *IEEE Trans. Veh. Technol.*, vol. 66, no. 5, pp. 3714–3723, May 2017.
[10] C. H. Kim, M. Y. Kim, and G. W. Moon, "A modularized charge equalizer using a battery monitoring IC for series-connected Li-ion battery strings in electric vehicles," *IEEE Trans. Power Electron.*, vol. 28, no. 8, pp. 3779–3787, Nov. 2013.
[11] C.-S. Lim, K.-J. Lee, N.-J. Ku, D.-S. Hyun, and R.-Y. Kim, "A modularized equalization method based on magnetizing energy for a series-connected lithium-ion battery string," *IEEE Trans. Power Electron.*, vol. 29, no. 4, pp. 1791–1799, Apr. 2014.
[12] Y. C. Hsieh, J. L. Wu, and X. H. Chen, "Class-E-based charge equalization circuit for battery cells," *IET Power Electron.*, vol. 5, no. 7, pp. 978–983, 2012.
[13] A. M. Imtiaz and F. H. Khan, "'Time shared flyback converter' based regenerative cell balancing technique for series connected Li-ion battery strings," *IEEE Trans. Power Electron.*, vol. 28, no. 12, pp. 5960–5975, Dec. 2013.
[14] C. Hua and Y.-H. Fang, "A charge equalizer with a combination of APWM and PFM control based on a modified half-bridge converter," *IEEE Trans. Power Electron.*, vol. 31, no. 4, pp. 2970–2979, Apr. 2016.
[15] C.-H. Kim, M.-Y. Kim, H.-S. Park, and G.-W. Moon, "A modularized two-stage charge equalizer with cell selection switches for series-connected lithium-ion battery string in an HEV," *IEEE Trans. Power Electron.*, vol. 27, no. 8, pp. 3764–3774, Aug. 2012.
[16] J.-W. Shin, G.-S. Seo, C.-Y. Chun, and B.-H. Cho, "Selective flyback balancing circuit with improved balancing speed for series connected lithium-ion batteries," in *Proc. Int. Power Electron. Conf. (ECCE ASIA)*, Jun. 2010, pp. 1180–1184.
[17] M. Arias, J. Sebastian, M. M. Hernando, U. Viscarret, and I. Gil, "Practical application of the wave-trap concept in battery–cell equalizers," *IEEE Trans. Power Electron.*, vol. 30, no. 10, pp. 5616–5631, Oct. 2015.
[18] Y. Shang, C. Zhang, N. Cui, J. M. Guerrero, and K. Sun, "A crossed pack-to-cell equalizer based on quasi-resonant LC converter with adaptive fuzzy logic equalization control for series-connected lithium-ion battery strings," in *Proc. IEEE Appl. Power Electron. Conf. Expo. (APEC)*, Mar. 2015, pp. 1685–1692.
[19] D. M. Yang, S. Y. Li, and G. D. Qi, "A bidirectional flyback cell equalizer for series-connected lithium iron phosphate batteries," in *Proc. 6th Int. Conf. Power Electron. Syst. Appl. (PESA)*, Hong Kong, 2015, pp. 1–5.
[20] T. H. Phung, J.-C. Crebier, A. Chureau, A. Collet, and V. Nguyen, "Optimized structure for next-to-next balancing of series-connected lithium-ion cells," in *Proc. 26th Annu. IEEE Appl. Power Electron. Conf. Expo. (APEC)*, Mar. 2011, pp. 1374–1381.
[21] F. Mestrallet, L. Kerachev, J.-C. Crebier, and A. Collet, "Multiphase interleaved converter for lithium battery active balancing," in *Proc. Appl. Power Electron. Conf. Expo.*, 2012, pp. 369–376.
[22] S. Li, C. Mi, and M. Zhang, "A high efficiency low cost direct battery balancing circuit using a multi-winding transformer with reduced switch count," in *Proc. 27th Annu. IEEE Appl. Power Electron. Conf. Expo. (APEC)*, Feb. 2012, pp. 2128–2133.
[23] C. Bonfiglio and W. Roessler, "A cost optimized battery management system with active cell balancing for lithium ion battery stacks," in *Proc. IEEE Vehicle Power Propuls. Conf.*, Sep. 2009, pp. 304–309.

[24] M. Chen, Z. Zhang, Z. Feng, J. Chen, and Z. Qian, "An improved control strategy for the charge equalization of lithium ion battery," in *Proc. 24th Annu. IEEE Appl. Power Electron. Conf. Expo.*, Feb. 2009, pp. 186–189.
[25] T. H. Phung, A. Collet, and J.-C. Crebier, "An optimized topology for next-to-next balancing of series-connected lithium-ion cells," *IEEE Trans. Power Electron.*, vol. 29, no. 9, pp. 4603–4613, Sep. 2014.
[26] C.-H. Lin, C.-H. Lin, H.-Y. Chao, and M.-H. Hung, "Dual-balancing control for improving imbalance phenomenon of lithium-ion battery packs," in *Proc. IEEE 3rd Int. Conf. Sustain. Energy Technol. (ICSET)*, Sep. 2012, pp. 229–234.
[27] Y.-S. Lee and M.-W. Cheng, "Intelligent control battery equalization for series connected lithium-ion battery strings," *IEEE Trans. Ind. Electron.*, vol. 52, no. 5, pp. 1297–1307, Oct. 2005.
[28] C. Pascual and P. T. Krein, "Switched capacitor system for automatic series battery equalization," in *Proc. IEEE Appl. Power Electron. Conf. Expo.*, Feb. 1997, pp. 848–854.
[29] S.-H. Park, T.-S. Kim, J.-S. Park, G.-W. Moon, and M.-J. Yoon, "A new battery equalizer based on buck-boost topology," in *Proc. 7th Int. Conf. Power Electron.*, Oct. 2007, pp. 962–965.
[30] C. Karnjanapiboon, K. Jirasereeamornkul, and V. Monyakul, "High efficiency battery management system for serially connected battery string," in *Proc. IEEE Int. Symp. Ind. Electron.*, Jul. 2009, pp. 1504–1509.
[31] J. Li, F. Gao, G. Yan, T. Zhang, and J. Li, "Modeling and SOC estimation of lithium iron phosphate battery considering capacity loss," *Protection Control Mod. Power Syst.*, vol. 3, no. 1, pp. 5–13, Dec. 2018.
[32] W. Waag, C. Fleischer, and D. U. Sauer, "Critical review of the methods for monitoring of lithium-ion batteries in electric and hybrid vehicles," *J. Power Sources*, vol. 258, pp. 321–339, Jul. 2014.
[33] D. V. Cadar, D. M. Petreus, and T. M. Patarau, "An energy converter method for battery cell balancing," in *Proc. IEEE 33rd Int. Spring Seminar Electron. Technol. (ISSE)*, May 2010, pp. 290–293.
[34] G. Yu, *Research on Bidirectional Equalization Strategy and System Development for Lithium-Ion Power Battery Pack of Pure Electric Vehicle*. Jilin, China: Jilin Univ., 2014, pp. 11–12.

YILIN CAO was born in Henan, China. She received the B.S. degree in electrical engineering and automation from Xuchang University, Henan, in 2018. She is currently pursuing the degree in mechanical engineering with the School of Mechanical and Electrical Engineering, Shihezi University, China. Her research interests include batteries management systems and power electronic converters.

KAI LI was born in Jiangsu, China. He received the degree from the School of Automation, Jiangnan University, Wuxi, China, in 2018. He is currently pursuing the Master of Engineering degree with the School of Mechanical and Electrical Engineering, Shihezi University, China. His current research interest includes the multi-motor coordination control systems.

MIN LU received the B.S. degree in control engineering from Xinjiang University, Xinjiang, China, in 2008, and the Ph.D. degree in electrical engineering from the Huazhong University of Science and Technology, Wuhan, China, in 2020. She is currently an Associate professor with Shihezi University. She mainly engaged in the reliability research of power electronics devices and the wind power generation technology.